Journal of Multidisciplinary Engineering Science and Technology (JMEST)
ISSN: 2458-9403
Vol. 7 Issue 4, April - 2020

Application of nitriding and duplex treatment on steel drills-HSS

Serra, P. L. C.
Department of Materials Engineering, Federal University of Piauí, Teresina, Brazil.
Federal University of Piauí, UFPI
Terezina, Brazil
plinniker@gmail.com

Sousa, R. R. M.
Department of Mechanical Engineering, Federal University of Piauí, Teresina, Brazil.
Federal University of Piauí, UFPI
Terezina, Brazil
romulorms@gmail.com

Barros Neto, J. R.
Department of Materials Engineering, Federal University of Piauí, Teresina, Brazil.
Federal University of Piauí, UFPI
Terezina, Brazil
joaorbneto@gmail.com

Libório, M. S.
School of Science and Technology, Federal University of Rio Grande do Norte, Natal, Brazil.
Federal University of Rio Grande do Norte, UFRN
Natal, Brazil
maxwellsantana@ect.ufrn.br

Feitor, M. C.
Department of Textile Engineering, Federal University of Rio Grande do Norte, Natal, Brazil.
Federal University of Rio Grande do Norte, UFRN
Natal, Brazil
Michelle_feitor@hotmail.com

Costa, T. H. C.
Department of Mechanical Engineering, Federal University of Rio Grande do Norte, Natal, Brazil.
Federal University of Rio Grande do Norte, UFRN
Natal, Brazil
thercioc@gmail.com

Furtado, A. S.
Department of Materials Engineering,
Federal University of Piauí, Teresina, Brazil.
Federal University of Piauí, UFPI
Terezina, Brazil
asfurtado@ufpi.br

***Abstract* — The present study aims to evaluate the application of plasma nitriding (at temperatures of 450° and 500°C) and duplex treatment (conventional nitriding followed by TiN deposition, using the cathodic cage deposition technique). Samples were characterized by Vickers Microhardness Test, Scanning Electron Microscopy-SEM, and Energy Dispersion Spectroscopy-EDS. Drill performance was evaluated after machining SAE1045 steel specimens, using flank wear and hole diameter measurements. The performance test pointed to the viability of the treatment at 450°C, whose treated drill had a longer life than in the untreated drill, in addition to meeting the dimensional quality in all holes. In contrast, the other tools, nitrided at 500°C and submitted to the duplex treatment, they presented performance below the expected, not showing viability for application in these conditions. Additionally, it was observed the existence of a thermal gradient formed during the treatment.**

Keywords—Plasma nitriding; duplex treatment; drills; high-speed steel (HSS); drilling

I. INTRODUCTION

Globalization drives companies to focus their efforts on reducing costs and increasing competitiveness. Growth data after the economic crisis, 2010-2017, show higher economic growth in countries with a focus on supply (optimization of production sectors)[1].

In manufacturing industries, increased competitiveness is related to the optimization of machining processes that can be achieved through two strategies: reduction of non-productive times (associated with passive times that involve human activity) and reduction of productive times [2]. The development of technologies to improve cutting tools contributes to the reduction of non-productive times through the manufacture of more resistant tools that make it possible to increase the interval between tool changes, and also in the reduction of productive times with the development of tools capable of working at higher cutting speeds or making fewer passes for the same machining operation [2], [3].

The use of carbide represented a significant advance in cutting tool technology. However, the high cutting speeds required by these tools limit their use in some operations, such as in the machining of small

diameter holes, which requires high rotation of the machines to reach the required speeds. Another limitation in the use of carbide is related to operations that require high toughness and resistance to flexing of tools, as in deep drilling. These limitations justify the widespread use of High-Speed Steel – HSS [4], [5].

An alternative to increase the hardness, wear-resistance, and life of the high-speed steel tools, while maintaining the high toughness of the core, consists of applying surface treatments [6]. One can highlight the plasma nitriding treatment, where the surface properties are modified through interaction with the plasma. This procedure is characterized by ease of control and reproducibility, in addition to being a non-polluting process, which is an essential feature given the need for environmental responsibility attributed to companies [7]–[9].

Another alternative to improve the tribological properties of tools is the application of high hardness coatings by physical vapor deposition - PVD. The deposition process associated with a preliminary nitriding treatment is called a duplex treatment and is more efficient for application to tools [9]. Nitriding produces a smoother transition between the hardness of the surface and that of the substrate, contributing to better adhesion of the deposited film [9], [10]. One of the most widely used coatings is TiN titanium nitride, which features high hardness, thermal stability, and abrasion resistance [11].

In this work, plasma nitriding treatments (with temperatures of 450 °C and 500 °C) and duplex treatment (conventional nitriding followed by deposition of titanium nitride - TiN) were applied in commercial high-speed steel drills. As comparison parameters, untreated high-speed steel drill and a coated commercial drill were used.

II. EXPERIMENTAL DETAILS

A. Materials

Eight helical drill-HSS without surface coating and two drills with surface coating were used. Following the classification of the Brazilian Association of Technical Standards [12], the drills are of type N, with a body length (helical part) of 81 mm, a total length of 125 mm, and a diameter of 9 mm. Each treatment was applied to two uncoated commercial drills, totaling six treated drills. The remaining tools were used as a comparison parameter.

B. Preparation of drills and cathodic cages

Before nitriding, the drills were subjected to chemical cleaning by immersion in a solution with 90% distilled water and 10% HCl for 100 s. Then they were washed in running water and immersed in a container with acetone in the ultrasound equipment for 20 min. The cathodic cages, used in the second stage of the duplex treatment, were sanded using 400 mesh sandpaper. Then they were immersed in a solution with 5% HF, 10% HNO_3, and 85% distilled water in the ultrasound equipment for 20 min. The cleaning was completed with washing under running water, followed by immersion in acetone for 1 min.

C. Conventional Nitriding

The treatments were carried out in a reactor that operates with a maximum alternating voltage of 800 V. Conventional nitriding was carried out at 450 °C and 500°C. These temperatures were chosen based on the work of Borgioli, Fossati, Galvanetto and Bacci [13] and Zagonel, Figueroa, Droppa and Alvarez [14], which showed greater better results of surface hardness for temperatures from 450 °C. The temperature was limited to 500 °C due to instability in the reactor during heating of the drills at higher temperatures. 600 V alternating voltage was used.

In the treatment at 450 °C, pre-sputtering was performed at 350 °C, with an atmosphere composed of 50% argon and 50% hydrogen, lasting 1 h, and pressure of 1 Torr. After this stage the temperature was raised to 450°C and the gas composition was changed to 75% hydrogen and 25% nitrogen, the pressure was increased to 3 Torr, maintaining these conditions for 5 h. Then the reactor was turned off and the drills were cooled to room temperature inside the vacuum chamber. In the second conventional nitriding treatment, the only difference was the treatment temperature, adjusted to 500 °C.

D. Duplex treatment

Duplex treatment is divided into two stages. The first is nitriding, carried out under the same conditions as the treatment at 500 ºC, described in the previous section. In the second stage, the deposition was performed using the cathodic cage deposition technique. The drills were positioned on an alumina disk and surrounded by a titanium cage. In the deposition, pre-sputtering was performed under the same conditions as conventional treatments. Then the temperature was raised to 500 ° C, and the atmosphere adjusted to make up 75% hydrogen and 25% nitrogen. The pressure used in the deposition was 1.24 Torr, which was the lowest possible within the equipment limitations. According to Bilek, Martin and McKenzie [15], efficiency of deposition increases with the reduction of treatment pressure. The conditions were maintained for 5 h. Then, the reactor was turned off, and the drills cooled to room temperature inside the vacuum chamber.

E. Nomenclature and preparation of samples for analysis

Table 1 shows the nomenclature adopted for the samples of each drill studied in this work, according to their characteristics.

TABLE I. NOMENCLATURE OF SAMPLES USEDD FOR ANALYSIS.

Samples	*Characteristics*
CWD	Commercial drill without coating
CCD	Coated commercial drill
N450	Nitrided at 450°C
N500	Nitrided at 500°C
Duplex	Duplex treatment at 500°C

In order to analyze the cross sections of the samples, they were cut in three regions along the body of the N450, N500, and CSR drills: close to the cutting edges (cut A), in the middle of the drill body (cut B) and at the junction between the body and the stem (cut C). Only a cross-sectional sample (cut A) was taken from the Duplex drill, considering that, according to Sousa et al. [16], there is no temperature gradient formation in parts kept at floating potential during cathodic cage treatment. In the CCD drill, only the region of section A was also studied, as this tool is used only as a comparison parameter and, therefore, studying the characteristics of its treatment is not the purpose of this work. In addition to the cross-sectional samples, a sample with the clearance surface was cut from each drill for the measurement of surface hardness.

F. Characterizations

The microhardness measurements on the Vickers scale were obtained using an INSIZE microdurometer model ISH-TDV 1000. Ten measurements were taken on the clearance surface of each sample to obtain an arithmetic mean. The load used was 0.2 kgf with an application time of 15 s. In order to analyze the hardness of the core of the transversal samples (cuts A, B and C), five measurements were made. The load used was 0.1 kgf with a time of 15 s. All measurements were performed following ASTM 1327-08 [17].

Metallographic observations were made using a Zeiss Optical Microscope (model AxioCam ICC 5 and software AxioVs40x64 V4.9.1.0) and a Scanning Electron Microscope - MEV Tescan (model Vega XMU). The polished surface was chemically etched with Nital 4% for 8 seconds.

The performance simulation was performed in a Numerical Command Machining Center - CNC, Romi - model D600.

For machining tests, SAE1045 steel was adopted, a medium carbon steel, of relatively low cost and widely used in industry [18], [19]. The specimen was modeled in the SolidWorks software, and its dimensions were determined according to the characteristics of deep drilling operation (depth of at least 5 times the diameter [4], [20]). The minimum distances between the holes, and the holes and the edges of the specimen were 1.5 times the hole diameter to avoid errors in the results [21].

At each machined block, 4 holes, the drill was removed to check for flank wear. An optical microscope model SZ-EWS-I007160 was used for image acquisition. Wear measurements were made using the free ImageJ software. Four stopping criteria were adopted: the maximum "V_{Bmax}" flank wear of 0.5 mm, the complete failure of the tool (including chipping of the cutting edge), the excessive occurrence of noise and the maximum number of 20 holes (due to the limited material for machining the proof bodies). The first one to be decisive

The hole diameters were measured using an Insize profile projector - model ISP-Z3015. The measurements were used to verify dimensional tolerance. According to the manufacturer of the tools used in this work, the minimum and maximum dimensions of the hole, according to the Brazilian Association of Technical Standards [22] are, respectively, 9,000 mm and 9,150 mm, for general use.

III. RESULTS AND DISCUSSION

Fig. 1 presents a graph with the sample mean and standard deviations of the microhardness measurements made on the clearance surface of the drills. The results show that the average hardness in the CCD drill (919.3 HV) is higher than that presented by CWD (772.0 HV), behavior expected by the presence of the surface coating. The three treatments caused an increase in surface hardness. In the N450 drill, the average surface microhardness was 14.83% higher than in the CSR drill. The N500 drill showed an average surface hardness of 978.8 HV. The increase due to treatment was 26.79%. This value even exceeded that presented by the CCD drill. The Duplex drill showed the highest value for the average surface hardness, reaching an average of 1030.6 HV, with a percentage increase of 33.50% about the starting material.

The increase in surface hardness with the increase in the treatment temperature agrees with the results obtained by Hiraoka, Watanabe and Umezawa [23] and Zagonel, Figueroa, Droppa and Alvarez [14]. Another consequence of the increase in temperature is the intensification of surface sputtering, which results in an increase in surface roughness [24]–[26], the most considerable dispersion of the microhardness measures of the N500 drill compared to the N450 may be related to this change.

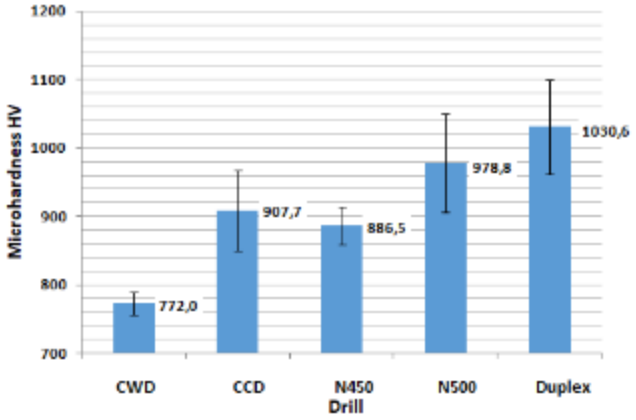

Fig. 1. *Microhardness on the clearance surface of the drills.*

The measurements of surface microhardness in the duplex drill resulted in an average of higher hardness than the N500. However, considering the error bars, these values are coincident. This dispersion was not expected in the measurements of surface microhardness in duplex drills because one of the objectives of applying TiN coatings is to reduce roughness [27] and according to De Sousa et al. [28] the uniformity of the deposited layer is one of the advantages of the cathodic cage deposition technique. This behavior may be related to the possibility of the indentations going beyond the deposited layer due to its small thickness, failing to measure the hardness of the film and measuring the hardness of the nitrided (non-uniform) layer formed in the first stage of treatment.

Fig. 2 shows the hardness measurements of the core in the three regions of the drills (cuts A, B, and C). In deposition using a cathodic cage, there is no temperature gradient over the length of the samples [28]. The nitriding of the duplex treatment was carried out under the same conditions as the treatment of the N500 drill. Therefore, the variation of properties in the cores of the Duplex and N500 drills are the same as those observed.

Fig. 2 shows a hardness decay in the core of the commercial drill, from 780 HV near the tip (cut A) to 437 HV at the junction between the body and the shank (cut C). This difference may be associated with a temperature gradient established during the tempering heat treatment, treatments known as “tailored tempering,” important for applications in which requests change in different regions. [29], [30]. Drills require considerable toughness close to the shank to avoid bending failure, and high hardness and wear resistance in the regions closest to the tip.

The hardness measurements shown in Fig. 2 show that the two temperatures applied in conventional nitriding caused a reduction in hardness in the core of the drills, which indicates the occurrence of tempering in the treatment. The graph indicates that at 450 °C the reduction was observed in cut A and at cut B. At 500 °C the reduction in hardness was seen in cut C. The reduction of hardness during tempering is known as tempering embrittlement. In conventional steels, the higher the temperature, the more significant the reduction in hardness due to tempering [31]. This progressive reduction was not observed in nitrided drills. In the N500 sample, a reduction in hardness is observed only in cut C, while in cut A the hardness of the substrate is the same as that of the untreated drill (CWD). This behavior is due to the secondary hardening caused by the precipitation of carbides from alloying elements to a temperature range that depends on the composition of the steel. [32].

The difference in sensitivity to tempering shown in Fig. 2, is related to the thermal gradient established. During plasma nitriding, sputtering is more pronounced at the top of the parts, causing higher heating in this region. Analyzing the results of the N450 drill, it is observed that the critical temperature for tempering is greater than 450 °C, since the reduction was not observed in the cut made close to the stem (cut C). In the N500 drill, it can be seen that the secondary hardening for the material occurs at temperatures above 500 °C, as in cut C there was a marked reduction in microhardness, while in cuts A and B no reduction in hardness was observed. These results show that the temperatures established in these regions are in the range where secondary precipitation hardening occurs.

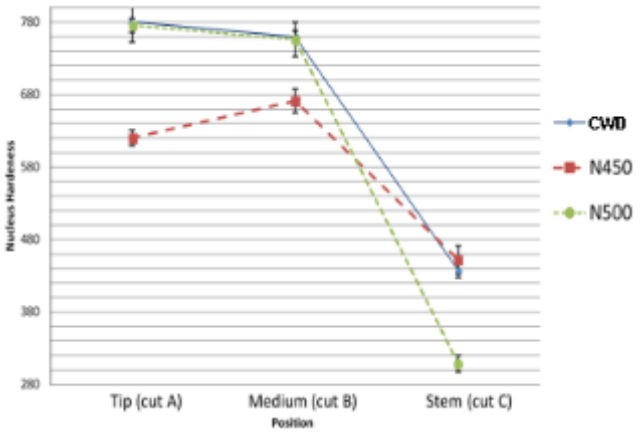

Fig. 2. Drill core hardness in cutting regions A, B, and C.

The occurrence of tempering during nitriding opens the possibility of simultaneous application of tempering and nitriding, which can contribute to the reduction of costs and manufacturing times, through the elimination of a processing step. Works such as de Prass, Fontana, and Recco [33] are beginning to study this alternative.

Fig. 3 shows the micrographs obtained in an optical microscope from transversal samples of commercial drills. The microstructure of the CWD drill shown in Fig. 3(a) is similar to the structure of the martensite, indicating that the drills must have undergone tempering treatment. Fig. 3(b) shows the CCD drill microscopy. The microstructure of the core of the treated bit is similar to tempered martensite,

which may mean that the bits have undergone tempering treatment followed by tempering.

EDS analysis of the CWD drill revealed the presence of silicon alloy elements - Si and chromium - Cr, as can be seen in Table 2. These alloy elements are directly related to the behavior shown in Fig. 2. The presence of "Si" raises the critical temperature of embrittlement by tempering, delaying the precipitation of retained austenite [31]. Chromium, on the other hand, allows a greater response to tempering, intensifying secondary hardening [32].

The cross-sectional sample of the CCD drill was subjected to analysis by EDS for a quantitative study of the chemical composition, shown in Table II. The electron beams were focused on points A and B represented in Fig. 4.

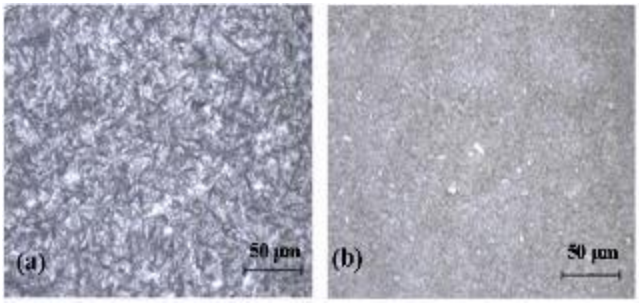

Fig. 3. Micrographs of transversal samples of commercial drills.

TABLE II. QUANTITATIVE EDS ANALYSIS OF THE UNCOATED COMMERCIAL DRILL – CWD.

Elements	*Weight (%)*	*Atom (%)*
Si	1.07	2.10
Cr	5.28	5.59
Fe	93.64	92.30

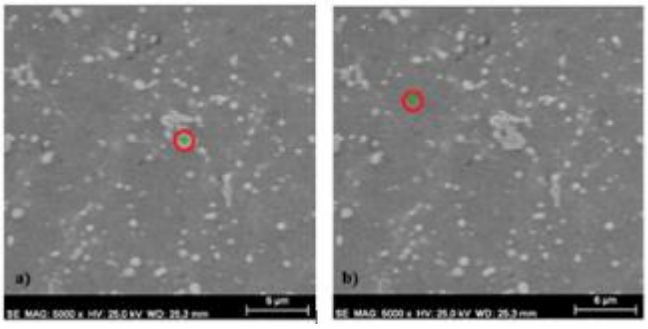

Fig. 4. Selected regions for EDS analysis.

TABLE III. QUANTITATIVE EDS ANALYSIS OF THE COATED COMMERCIAL DRILL – CCD (COMPOSITION AT POINT A AND B REPRESENTED IN FIG.4).

Point	*Element*	*Weight (%)*	*Atom (%)*
A (precipitate)	V	6.81	10.66
	Cr	3.77	5.77
	Fe	36.15	51.58
	Mo	22.41	18.61
	W	30.86	13.37
	Total	100	100
B (Matrix)	V	1.36	1.62
	Cr	4.65	5.40
	Fe	80.31	86.90
	Mo	5.26	3.31
	W	8.42	2.77
	Total	100	100

The results of EDS prove that the region of point A is a precipitate of carbides, formed mainly by tungsten and molybdenum. The precipitation of these carbides, which probably occurred during tempering, is characteristic of high-speed steels and is responsible for their secondary hardening. These carbides, in addition, to increase hardness, increase wear resistance [34], [35]. Point B has predominantly iron with the elements of tungsten, molybdenum, vanadium, and chromium alloys dissolved. The combination of alloy elements dissolved in the tempered iron matrix and precipitates, mainly of tungsten and molybdenum, justify the high hardness measured in the core of the CCD drill compared to CWD.

Fig. 5 shows the micrograph of the cross-sections (sections A, B, and C) obtained along the body of the nitrided drills at 450 and 500 ° C.

Looking at Fig. 5, it can be seen that the layer of compounds was formed under the two nitriding conditions in all analyzed regions. The N450 drill layer is more uniform than the N500. Uniformity decreases towards the tip of the drills. According to De Araújo et al. [8], when nitriding higher parts, the sputtering rate is higher on the upper surface. This difference is due to the direction of movement of the active plasma species, resulting in more uniform layers on the lateral surface of these parts. We can observe that with the increase in the treatment temperature, the uniformity of the layers decreases when comparing Fig. 5 (e) with Fig. 5 (f), this result is in line with those presented by Aguajani, Torshizi, and Sol notarh [36].

Fig. 6 shows the micrograph of the transversal sample of the drill submitted to the duplex treatment. The cross-section was made close to the tip of the tool.

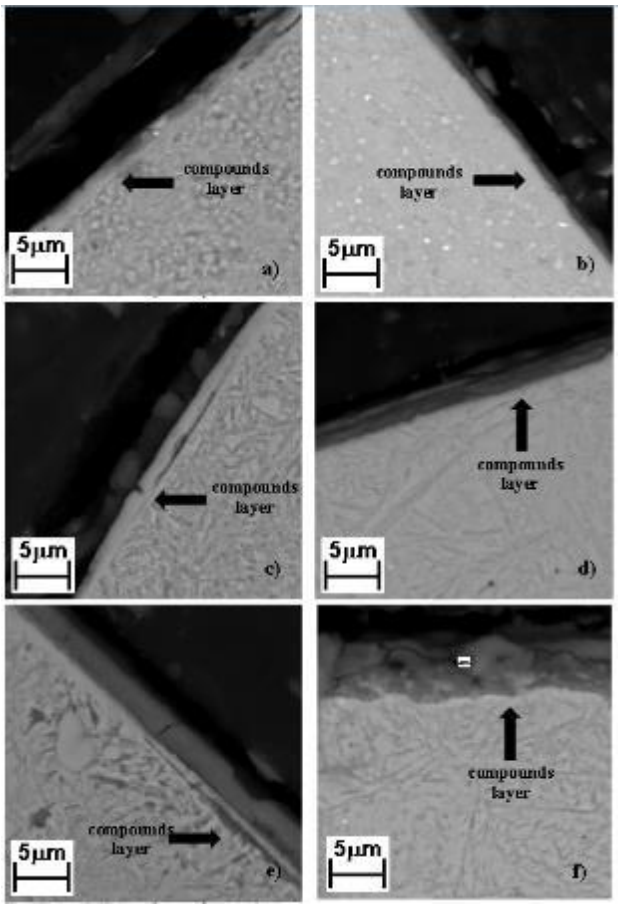

Fig. 5. Micrograph of the croos-sections (cuts A, B, and C) of the N450 and N500 drills.

In Fig. 6 it is possible to observe the thin layer deposited just above the nitride layer, the irregularities on the surface originate from conventional nitriding at 500 °C, carried out in the first stage of the treatment and, also, it is influenced by the sample cutting process. The N500 drill layer shown in Fig. 5(f) has a similar appearance.

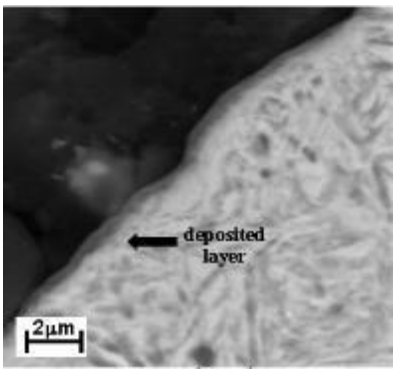

Fig. 6. MEV of the cross-section (cut A) of the CCD drill.

Tab. IV shows the thickness measurement of the layers shown in Fig. 5, and Fig. 6.

In Table IV, the variation in the layer thickness along the body of the drills submitted to conventional nitriding is observed, so that the thickness grows from the stem to the tip, this behavior is associated with the thermal gradient that was evidenced in the microhardness results and previously studied in the work of Lima et al. [37]. The increase in temperature in the same direction justifies the increase in layer thickness [36], [38]. The variation in the thickness of the layer is also due to the geometry of the drill, which has a much larger lateral surface than the frontal one, which results in greater layer thicknesses in the regions closest to the upper surface of the parts, similar behavior was observed by De Araújo et al. [8]

TABLE IV. THICKNESS MEASUREMENTS OF THE COMPOUND LAYER IN THE NITRIDED DRILLS AT 450 AND 500 °C AND THE THIN FILM IN THE DRILL SUBJECTED TO DUPLEX TREATMENT AT 500 °C.

Treatment	*cut*	*Compound layer thickness (µm)*	*Thin film thickness (µm)*
Nitrided at 450 °C	Tip (A)	2.80	-
	Medium (B)	1.94	-
	Stem (C)	1.22	-
Nitrided at 450 °C	Tip (A)	5.78	-
	Medium (B)	2.50	-
	Stem (C)	0.86	-
Duplex (500 °C)	Tip (A)	-	0.64

Regarding the two nitriding conditions, it is observed that in the upper regions (section A and B), the layer thickness measurements in the N500 drill were higher than in N450, showing once again that the thickness increases with temperature. The measurements in the region close to the stem (cut C) did not show the same trend. Therefore, this result may have been influenced by the drill geometry, due to the possibility of variation of the angle of incidence of the ions in the region of the edges, not affecting the surface perpendicularly. , causing a proportional decrease in the sputtering rate. Sputtering is one of the main mechanisms of the formation of the nitride layer. Therefore, its decrease is reflected in the formation of thinner layers [8].

The nitrided drill at 500 ºC showed the worst result in the performance test, failing before the first hole

was completed. Fig. 7 shows the drill after interrupting the test.

Analyzing Fig. 7, it can be seen that there was chipping of the cutting edge, which caused an imbalance in the drilling process accompanied by an increase in the noise level. Chipping in this region can be associated with local hardening due to the high treatment temperature and edge effect (concentration of charges on the edges of the tool that cause higher heating in these regions) that is characteristic of conventional nitriding. This effect becomes more critical as the treatment temperature increases, producing less uniform layers [8], as was observed in the scanning electron microscopy presented in Fig. 5 and in the dispersion of the microhardness measurements in Fig. 1.

The results of flank wear of the CWD, CCD, N450, and Duplex drills as a function of the number of holes drilled are shown in Fig. 8. The result does not include the N500 drill because it failed in the first hole.

Fig. 7. Chipping of the cutting edge in the nitrided drill at 500 °C – N500.

The behavior of the N450, CWD, and CCD drills was similar in some aspects. The tools initially showed a higher wear rate in the first 4 holes and then maintained an approximately constant rate until holes 12, 16, and 20 for the CWD, N450, and CCD drills, respectively.

The commercial drill without coating showed satisfactory performance up to 14 ° hole when the machining was interrupted due to the high noise level, which according to Miranda, Santos, Kieckow, and Casarin [4], is related to the presence of the adhesion wear mechanism, as can be seen—seen in Fig. 9, combined with high flank wear. The CWD drill showed adhesion wear, as can be seen in Fig. 9.

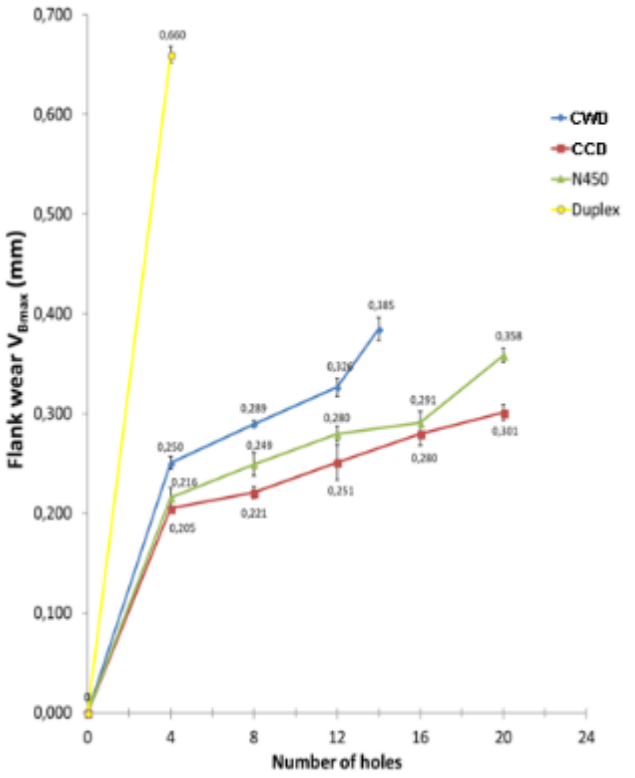

Fig. 8. Flank wear as a function of number of holes in the CWC, CCD, N450, and Duplex samples.

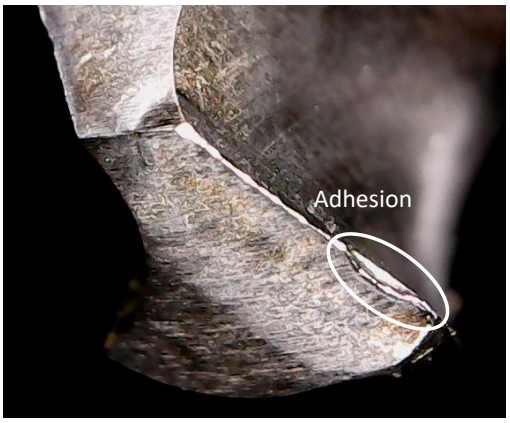

Fig. 9. Adhesive and flank wear observed in the uncoated commercial drill – CWD.

Fig. 8 shows that the N450 and CCD drills machined the maximum number of predicted holes (20 holes) without reaching the end of their service life. Nitriding at 450 °C increased the resistance to flank wear compared to the starting material, since after machining the 20° hole, the flank wear shown (0.358 mm) was still less than that shown by the CWD drill bit, which already had high flank wear (0.385 mm) in the 14th hole. In the 16th hole, the wear of the N450 drill was only 0.291 mm. This result is due to the increase in hardness caused by nitriding and the more excellent uniformity of the layer in relation to the treatment at 500 ºC, decreasing the level of internal stresses.

In comparison to the CCD drill, the flank wear shown by N450 was higher. However, both showed similar results up to the 16th hole. In the measurements made after the 4th and the 16th hole, the wear coincides when considering the deviation of the measurements. The better behavior of the CCD drill can be attributed to the uniformity of its surface coating. Additionally, of all tested drills, it was the one that showed the least dispersion in the microhardness results and the lowest noise level during machining, which may be related to low surface roughness and low friction in the tool/part contact [39].

The drill submitted to the duplex treatment did not present satisfactory performance, only 4 holes were drilled, and the stop criterion was the maximum flank wear equal to 0.660 mm (exceeding the 0.5 mm limit), as shown in Fig. 8. The poor performance may be associated with poor adhesion of the film or the superficial roughness of the duplex bur (originated in the first stage of treatment), which was suggested by the dispersion of the microhardness results in Fig. 1. According to Lima and Ferraresi [39], the higher the roughness, the less the resistance to abrasive wear.

Fig. 10 shows the values of the hole diameter measurements, and the maximum and minimum allowable diameters according to the Brazilian Association of Technical Standards [22], for the dimensional tolerance defined for drilling operations in general. The results of the CWD, CCD, N450, and Duplex drills are presented. The N500 drill does not appear in the results because it failed before the first hole was completed. The results in Fig. 10 show that the best results were achieved with the N450 drill, the only one that machined all the holes within the tolerance recommended for machining conditions like high-speed steel drills [22].

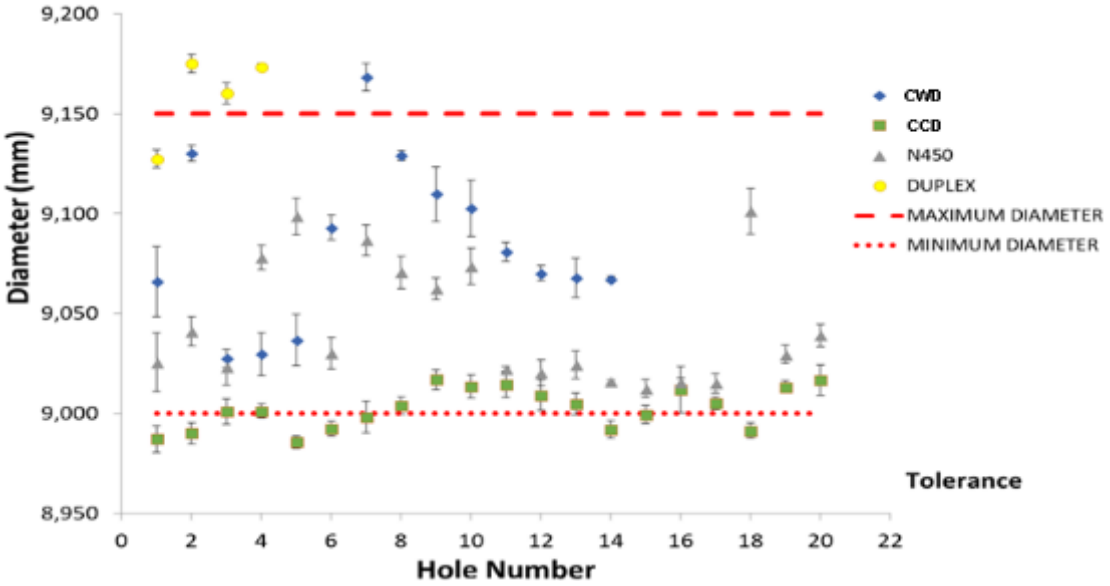

Fig. 10. Hole diameter based on technical standard [22].

The CCD drill had the smallest diameters, but for the machining, condition applied, it was not adequate, as it machined holes below 9.00 mm, that is, out of dimensional tolerance. This behavior as well, and the low abrasive wear shown in Fig. 8 indicate low roughness of the coating, which facilitates the chip to exit, resulting in smaller diameter holes. The increase in cutting speed would contribute to the machining of larger holes, but would increase the flank wear, and may even exceed that presented by the N450 drill. [22].

The duplex drill again showed an unsatisfactory result. Among the 4 machined holes, only 1 met the dimensional tolerance and the others had diameters larger than the maximum allowable. The increase in the diameter of the holes may be related to an imbalance caused by the uneven wear of the cutting edges of the tool during machining. This difference is shown in Fig. 11.

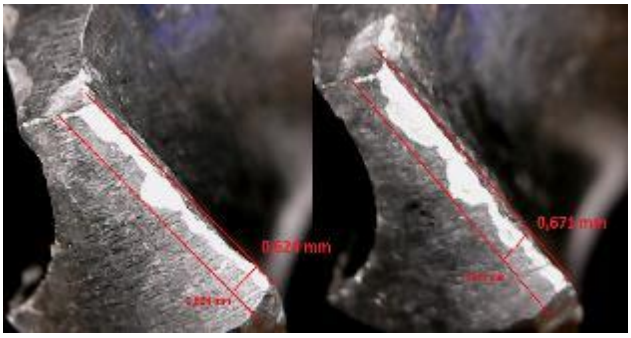

Fig. 11. Wear of the cutting edges of the Duplex sample.

IV. Conclusion

The results showed the effectiveness of the application of plasma nitriding in increasing the surface hardness of HSS drill bits. It was observed that the hardness increases with the increase in the treatment temperature.

In relation to the other treatments, the treatment at 450 °C produced more uniform layers. The uniformity of the layer is observed in the regions distant from the tip and closer to the stem, while the thickness increases in the opposite direction.

For the machining of SAE 1045 steel, the bit nitrided at 450 °C - N450, presented the best performance among all tested bits, contributing to the increase of tool life and the improvement of dimensional quality in deep drilling operations.

V. ACKNOWLEDGEMENTS

This work was partially supported by the Brazilian agency, CAPES.

REFERENCE

[1] D. Hoffmann and M. Alcino Ribeiro da Fonseca, “The impact of the financial crisis in Brazil and Germany: A comparative analysis of distinct developments The impact of the financial crisis in Brazil and Germany,” 2011.

[2] E. A. Baptista and N. Lemos Coppini, “MAXIMIZANDO O LUCRO: OTIMIZANDO PROCESSOS DE USINAGEM COM AUXÍLIO DE SISTEMA ESPECIALISTA.”

[3] S. V Bhaskar and H. N. Kudal, “Archives of Mechanical Technology and Materials Tribology of nitrided-coated steel-a review,” *Arch. Mech. Tech. Mater*, vol. 37, pp. 50–57, 2017.

[4] E. Miranda, D. Santos, F. Kieckow, and J. J.Casarin, “AVALIAÇÃO DO DESGASTE DE BROCAS HELICOIDAIS DE AÇO-RÁPIDO (HSS) MODIFICADAS SUPERFICIALMENTE POR NITRETAÇÃO A PLASMA Evaluation of Wear High Speed Steel Twist Drill Superficially Modified by Plasma Nitriding,” *reitoria.uri.br*, vol. 9, pp. 68–76, 2013.

[5] D. Whan Kim, Y. Soo Lee, M. Soo Park, and C. Nam Chu, “Tool life improvement by peck drilling and thrust force monitoring during deep-micro-hole drilling of steel,” *Elsevier*, 2008.

[6] V. M. Kishurov, V. N. Ippolitov, M. V. Kishurov, and M. Y. Nekrasova, “Influence of wear-resistant coatings on tool performance,” *Russ. Eng. Res.*, vol. 32, no. 2, pp. 182–185, Feb. 2012.

[7] M. Quast, H. R. Stock, and P. Mayr, “Plasma-assisted nitriding of aluminum-alloy parts,” in *Metal Science and Heat Treatment*, 2004, vol. 46, no. 7–8, pp. 299–304.

[8] F. O. De Araújo, ; R S De Sousa, ; A K G De Araújo, ; K J B Ribeiro, and ; C Alves, “NITRETAÇÃO A PLASMA DE AÇO INOXIDÁVEL AUSTENITICO AISI 316: UNIFORMIDADE DA CAMADA NITRETADA,” 2007.

[9] A. Rousseau, J. Partridge, … E. M.-S. and coatings, and undefined 2015, “Microstructural and tribological characterisation of a nitriding/TiAlN PVD coating duplex treatment applied to M2 High Speed Steel tools,” *Elsevier*.

[10] M. Naeem, M. Shafiq, M. Zaka-ul-Islam, J. D.-G.-M. Letters, and undefined 2017, “Improved surface properties of AISI-304 by novel duplex cathodic cage plasma nitriding,” *Elsevier*.

[11] M. Bashir, M. Shafiq, M. Naeem, … M. Z.-I.-S. and C., and undefined 2017, “Enhanced surface properties of aluminum by PVD-TiN coating combined with cathodic cage plasma nitriding,” *Elsevier*.

[12] S. Rocha, “Avaliação do desempenho de brocas helicoidais de aço rápido revestidas na usinagem de ferro fundido nodular GGG50,” 2012.

[13] F. Borgioli, A. Fossati, E. Galvanetto, and T. Bacci, “Glow-discharge nitriding of AISI 316L austenitic stainless steel: Influence of treatment temperature,” *Surf. Coatings Technol.*, vol. 200, no. 7, pp. 2474–2480, Dec. 2005.

[14] L. F. Zagonel, C. A. Figueroa, R. Droppa, and F. Alvarez, “Influence of the process temperature on the steel microstructure and hardening in pulsed plasma nitriding,” *Surf. Coatings Technol.*, vol. 201, no. 1–2, pp. 452–457, Sep. 2006.

[15] M. Milena, M. Bilek, P. J. Martin, D. R. Mckenzie, M. M. M. Bilek, and P. J. Martin, “Influence of gas pressure and cathode composition on ion energy distributions in filtered cathodic vacuum arcs,” *Artic. J. Appl. Phys.*, vol. 83, no. 6, pp. 2965–2970, Mar. 1998.

[16] R. R. M. de Sousa, F. O. de Araújo, K. J. B. Ribeiro, M. W. D. Mendes, J. A. P. da Costa, and C. Alves, “Cathodic cage nitriding of samples with different dimensions,” *Mater. Sci. Eng. A*, vol. 465, no. 1–2, pp. 223–227, Sep. 2007.

[17] C. A.-A. B. of A. Standards and undefined 2008, “1327–08. Standard test method for Vickers indentation hardness of advanced ceramics.”

[18] K. Gu *et al.*, “Electrochemical corrosion and impedance study of SAE1045 steel under gel-like environment,” *Elsevier*.

[19] A. Qasim, S. Nisar, A. Shah, … M. K.-… M. P. and, and undefined 2015, “Optimization of process parameters for machining of AISI-1045 steel using Taguchi design and ANOVA,” *Elsevier*.

[20] F. Marques, … A. R.-R., and undefined 2015, "Caracterização de desgaste de brocas de HSS revestidas com AlCrN e não revestidas, em ensaios de furação, na usinagem de ferro fundido nodular DIN GGG 50," *search.proquest.com*.

[21] J. Robert Pereira Rodrigues, T. do Espírito Santo Baldez Neves, M. Bacci da Silva, K. Carlos Ribeiro Martins, J. Ribamar dos Santos Ribeiro, and A. Pereira Andrade Cunha, "Acta Scientiarum Study of the application of sunflower oil in the process of drilling ABNT 1045 steel," *periodicos.uem.br*, vol. 36, no. 2, pp. 257–262.

[22] N. A. J. A. B. de N. Técnicas and undefined 1995, "6158. Sistema de tolerâncias e ajustes."

[23] Y. Hiraoka, … Y. W.-J. O., and undefined 2016, "Effect of Nitriding Temperature and Compositions on Diffusion Layer's Hardness in Gas Nitrided Low Alloy Steel Containing Chromium," *… INST Met. Mater. 1-14 …*.

[24] S. Hosseini, A. A.- Vacuum, and undefined 2013, "Evaluation of the effects of plasma nitriding temperature and time on the characterisation of Ti 6Al 4V alloy," *Elsevier*.

[25] D. She, W. Yue, Z. Fu, C. Wang, X. Yang, and J. Liu, "Effects of nitriding temperature on microstructures and vacuum tribological properties of plasma-nitrided titanium," *Surf. Coat. Technol.*, vol. 264, pp. 32–40, 2015.

[26] Y. Li, W. Wang, B. Hu, Y. He, J. Xiu, and Y. Zhu, "Wear and corrosion properties of AISI 420 martensitic stainless steel treated by active screen plasma nitriding Plasma Nitriding of Stainless Steel View project Wear and corrosion properties of AISI 420 martensitic stainless steel treated by active screen plasma nitriding," *Elsevier*, 2017.

[27] M. Ali, E. Hamzah, and M. R. Toff, "Friction coefficient and surface roughness of TiN-coated HSS deposited using cathodic arc evaporation PVD technique," *Ind. Lubr. Tribol.*, vol. 60, no. 3, pp. 121–130, 2008.

[28] R. Ribeiro *et al.*, "Uniformity of temperature in cathodic cage technique in nitriding of austenitic stainless steel AISI 316," *Taylor Fr.*, vol. 24, no. 4, pp. 313–318, Jul. 2008.

[29] M. Merklein and T. Svec, "Hot stamping: Manufacturing functional optimized components," *Prod. Eng.*, vol. 7, no. 2–3, pp. 141–151, 2013.

[30] G. M. Zapata, "UNIVERSIDADE ESTADUAL DE CAMPINAS Faculdade de Engenharia Mecânica Estudo da Decomposição da Austenita na Estampagem a Quente de Aços Endurecíveis ao Boro para Obtenção de Produtos com Propriedades Mecânicas Customizadas," [s.n.], 2017.

[31] J. Marcomini, H. G.-T. em M. e Materiais, and undefined 2012, "New Fe-C-Mn-Si-Cr bearing alloy: tempering curves and tempered martensite embrittlement/Nova liga Fe-C-Mn-Si-Cr para rolamentos: curvas de revenimento e," *go.gale.com*.

[32] C. E. Pinedo, "TRATAMENTO TÉRMICO E SUPERFICIAL DO AÇO INOXIDÁVEL MARTENSÍTICO AISI 420 DESTINADO A MOLDES PARA INJEÇÃO DE POLÍMEROS PARTE I-TRATAMENTO TÉRMICO 1."

[33] A. Prass, L. Fontana, A. R.-M. (Rio de Janeiro), and undefined 2017, "Nitretação por plasma com revenimento simultâneo do aço ferramenta VF 800AT," *SciELO Bras.*

[34] C. E. Pinedo and W. A. Monteiro, "Influence of heat treatment and plasma nitriding parameters on hardening martensitic stainless steel AISI 420/Tratamento termico e de nitretacao sob plasma do aco inoxidavel martensitico AISI 420," *Tecnol. em Metal. e Mater.*, vol. 8, no. 2, pp. 86–91, Apr. 2011.

[35] W. Santos, J. P. Neto, … R. S.-M. (Rio, and undefined 2015, "Desenvolvimento de dispositivo e estudo do comportamento ao microdesgaste abrasivo do aço AISI 420 temperado e revenido," *SciELO Bras.*

[36] H. Aghajani, M. Torshizi, M. S.- Vacuum, and undefined 2017, "A new model for growth mechanism of nitride layers in plasma nitriding of AISI H11 hot work tool steel," *Elsevier*.

[37] J. A. Lima and C. Alves, "Estudo do gradiente térmico no processo de nitretação a plasma."

[38] P. Cavaliere, A. Perrone, A. S.-E. S. and Technology, and undefined 2016, "Multi-objective optimization of steel nitriding," *Elsevier*.

[39] A. Lima, V. F.-S. & Inspeção, and undefined 2009, "Análise da microestrutura e da resistência ao desgaste de revestimento duro utilizado pela indústria sucroalcooleira," *SciELO Bras.*